Journal of Surgical Oncology 1999;71:189–195

Distribution of Gland-Like Structures in Human Gallbladder Adenocarcinomas Possesses Fractal Dimension

PRZEMYSLAW WALISZEWSKI, MD, PhD*
Department of Colorectal Surgery and Department of Cancer Biology, The Cleveland Clinic Foundation, Cleveland, Ohio

Background and Objectives: Epithelial cells form tissue patterns of higher order such as gland-like structures. A question arises whether distribution of those patterns in adenocarcinomas is subject to certain regularity.
Methods: Due to the pilot nature of this study, gallbladder adenocarcinomas were preselected by histopathological, immunohistochemical, and morphometric analysis to ensure relative homogeneity of the patterns analyzed. A box-counting method was applied to investigate a relationship between a number of gland-like structures and a radius of the expanding family of the concentric circles.
Results: The coefficient of linear regression characterizing that relationship possesses noninteger value. It is 1.585 (well-differentiated adenocarcinomas, standard deviation (SD) = 0.038, n = 100 sections), and 1.340 (moderately differentiated adenocarcinomas, SD = 0.044, n = 100 sections). While both nuclear area and nucleo-cytoplasmic ratio in those tissues remain within a similar range (Analysis of Variance (ANOVA), $F^0 = 0.791 < F_\alpha = 3.84$, $P = 3 \times 10^{-3}$ and $F^0 = 0.077 < F_\alpha = 3.84$, $P = 10^{-6}$, respectively, for k = 20,000 cells, in which F^0 is a value of the test function, F_α is a critical, limit value of the F-test at the constant confidence value $\alpha = 0.05$), a difference of fractal dimension is significant ($F^0 = 3.94 > F_\alpha = 0.693$, n = 100 sections, $P = 2 \times 10^{-3}$). Also, variablity of fractal dimension between tumor sections is significant (moderately differentiated adenocarcinomas, $F^0 = 1.9856 > F_\alpha = 1.4262$, n = 100 sections, $P = 0.189$).
Conclusions: There is fractal regularity in distribution of gland-like structures in human gallbladder adenocarcinomas. Fractal dimension is a holistic parameter which can be applied to evaluate tumor grading in a quantitative manner. *J. Surg. Oncol. 1999:71:189–195.*

KEY WORDS: complexity; fractal; fractal dimension; image analysis; adenocarcinomas; gallbladder neoplasia

INTRODUCTION

Either normal or transformed epithelial cells form a variety of morphological patterns of higher order (i.e., gland-like structures, crypt-like structures, cords, bundles, rossettes, or compact plaques, etc.). Given that there is geometrical self-similarity of the morphological patterns between normal-appearing mucosa and the corresponding adenocarcinomas [1–3], and that the macroscopic borders of adenomas and adenocarcinomas possess noninteger dimension [4], the existence of a fractal dimension in the distribution of those patterns is likely [5].

*Correspondence to: Przemyslaw Waliszewski, MD, PhD, Os. Jana III Sobieskiego 41 m. 21, 60-688 Poznan, Poland.
E-mail: WaliszP@amu.edu.pl
Accepted 3 April 1999

This work has been undertaken as a pilot study to test the hypothesis that distribution of gland-like structures in gallbladder adenocarcinomas possesses fractal regularity (i.e., by definition, this distribution is scale-invariant, either self-affine (the anisotropic rescaling) or self-similar (the isotropic rescaling), can be reconstructed as a union of rescaled copies of itself, or have noninteger, fractal dimension). More specifically, the study was performed to: 1) obtain an estimate of the mean and the standard deviation (SD) of fractal dimension for future pragmatic study [6,7]; 2) to determine fractal dimension in different areas of the same tumor; 3) to compare fractal dimension of well-differentiated (G1) and moderately differentiated (G2) adenocarcinomas. Due to the explanatory nature of this study, an effort has been made to control potential sources of extraneous variation and to compare relatively homogenous groups of tissues.

The method applied counts a number of gland-like structures within a grid of an expanding family of concentric circles, i.e., the circles centered at a given point with the radius increasing in a constant manner, and upon calculating whether the numbers fit a linear regression curve. This procedure is justified by the fact that fractal has the algebraic equivalent of the general form $y = ax^b$ called power law, where y is a number of objects counted in the single circle, x stands for a radius of the circle, a is a scaling coefficient, and b is the noninteger fractal dimension. This equation can be transformed to the linear function, (i.e., $\log y = b \log x + \log a$). The slope b of the latter function called the function of linear regression is identical to the dimension of the space occupied by the patterns analyzed [8].

The results show that distribution of gland-like structures in human gallbladder adenocarcinomas does possess fractal dimension. There is a variability of the parameter between consecutive sections of the same tumor. A significant difference exists between well-differentiated and moderately differentiated adenocarcinomas.

MATERIALS AND METHODS

Materials

The gallbladder adenocarcinomas selected for this study comprised 10 well-differentiated adenocarcinomas (G1) and 10 moderately differentiated adenocarcinomas (G2). All specimens were taken from the bottom of the female gallbladder. The average age of patients was 60.5, range 53–65 and 63.1, range 58–71, for adenocarcinomas (G1) and (G2), respectively. Tissue samples were obtained from the Department of Morbid Anatomy, The London Hospital in London, United Kingdom, and from the Department of Clinical Pathomorphology, University Medical School in Poznan, Poland. Histopathological typing of lesions was performed according to the World Health Organization system [1].

To construct relatively homogenous groups of gallbladder adenocarcinomas, a number of tumors previously enrolled in the data bank as well-differentiated adenocarcinomas (G1) or moderately differentiated adenocarcinomas (G2) were carefully reexamined. Tumor cells had to be neutral mucin-positive, N-acetylsialomucin-positive, sulphomucin-negative, O-acetylsialomucin-negative, and CEA-positive, where distribution of the antigens was glandular, (i.e., the antigens were present within a lumen of the gland-like structure) or apical (i.e., the antigens were dispersed along the luminal surface of cells in the gland-like structure) [9–13]. A pattern was classified as a well-differentiated adenocarcinoma (G1) if it was composed of well-formed small glands similar to those in normal mucosa. A pattern containing mainly both well-formed and poorly formed glands with few solid cords of cells was defined as a moderately differentiated adenocarcinoma (G2). The pattern was classified as a poorly differentiated adenocarcinoma (G3) if the pattern was mainly composed of solid cords of cells or cells dispersed in the stroma and few poorly formed glands. In the latter case, such a tumor was excluded from the study. Furthermore, the gland-like structures had to possess a size of a similar range and to be present in a number high enough to facilitate both measuring and calculations. Tissues with large areas infiltrated by cancer cells or lymphocytes; with necrosis, or a very low number of the gland-like structures (less than 20); or those with patterns of enlarged and branched glands were also excluded from the study. Ten consecutive tissue sections were taken from each tumor at approximately every 20 μm. The morphometrical parameters such as nucleo/cytoplasmic ratio (N/C) and nuclear area of cells (NA) were determined to ensure the relative cellular homogeneity between sections, and, finally, fractal analysis was performed.

Histochemistry

Samples were fixed in 10% buffered formalin and embedded into paraffin. The material was cut into 3–4-μm sections. The slides were stained with hematoxylin-eosin. Subsequently, series of deparaffinized sections were stained with diastase/alcian blue, pH 2.5/periodic acid-Schiff (D/AB, pH 2.5/PAS), periodic acid-borohydride/kalium hydroxide/PAS (PB/KOH/PAS), high-iron diamine/alcian blue, pH 2.5 (HID/AB, pH 2.5) (Sigma, St. Louis, MO) as described by Culling et al. [14]. Colonic mucosa was used as a positive control. Umbilical cord was used as a negative control. Results were interpreted according to Table I.

TABLE I. A Summary of Reagents and Color Reactions Used to Analyze Mucin Profile of Gallbladder Adenocarcinomas

	D/AB pH, 2.5/PAS	PB/KOH/PAS	HID/AB
Neutral mucins	Red	ND	ND
N-acetylsialomucins	Blue	ND	Blue
Sulphomucins	Blue	ND	Brown
O-acetylsialomucins	Blue	Red	Blue

D/AB pH, 2.5/PAS, diastase/alcian blue, pH 2.5/periodic acid-Schiff; PB/KOH/PAS, periodic acid-borohydride/kalium hydroxide/PAS; HID/AB pH 2.5, a mixture of high-iron diamine/alcian blue, pH 2.5; ND, nondetected.

Immunohistochemistry

The indirect immunoperoxidase technique was applied as described by Culling et al. [14]. Briefly, deparaffinized sections were treated with 3% H_2O_2 to block endogenous peroxidase activity, washed in phosphate buffer (PBS), and then blocked in normal swine serum diluted 1:20 in 1% bovine serum albumin-PBS for 30 min. Following this step, the polyclonal rabbit antibodies, anti-CEA (Dako, Copenhagen, Denmark) diluted 1:100 were applied for 1 hr at room temperature. After washing for 10 min in PBS, the sections were incubated with swine-anti-rabbit IgG (1:50). After incubation, the sections were rinsed in PBS and then treated with peroxidase-antiperoxidase complex (1:100) for 30 mins at room temperature. The peroxidase was developed with 0.03% H_2O_2 and 0.05% diaminobenzidine tetrahydrochloride dihydrate for 5 mins. When this step was complete, the slides were rinsed in water, counterstained with hematoxylin, dehydrated, and mounted in Canadian balsam.

Morphometrical Analysis

Morphometrical analysis was performed on hematoxylin-eosin-stained histological sections by the semiautomatic computerized image acquisition and analysis system: light microscope (Nikon, Tokyo, Japan), CCD camera (Hitachi, Tokyo, Japan), and image software package (Adobe Systems Inc., Mountain View, CA) with frame graber of 512 × 512 pixels installed upon PC computer. Human red blood cells were used for scaling of the image analyzer. The sections were studied under a microscope. The image of the microscopic field was analogue–digital converted and projected onto the monitor screen. Nucleo/cytoplasmic ratio (N/C) and nuclear area (NA) were measured as described [1,2]. Briefly, N/C ratio was calculated by measuring the outline of an area containing an average of 20 cells and the outline of each nucleus included in this area. In each case, 10 areas were measured within a given histological compartment. NA was calculated by measuring the outlines of longitudinally sectioned nuclei. Subsequently, fractal dimension was determined for the same compartment.

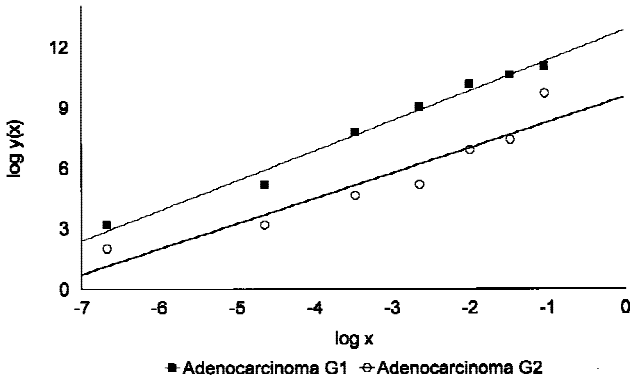

Fig. 1. A typical log-log plot of the number y(x) of gland centers within a distance x of a typical gland in a two-dimensional section. A square root of 2 was used as a base of all logarithms. The full squares correspond to the series of numbers obtained for a section of the well-differentiated adenocarcinoma G1. The line is a curve of the linear regression with the slope $F_D = 1.489$; SD = 0.084; t = 17.654; $P = 0.0001$; R = 0.992. Similarly, the circles correspond to the series of numbers obtained for a section of the moderately differentiated adenocarcinoma G2. The curve of the linear regression has the slope $F_D = 1.256$; SD = 0.198; t = 6.348; $P = 0.0014$; R = 0.943.

Fractal Analysis

The gland-like structures were recorded in a 20× visual field by the same semiautomatic computerized image acquisition and analysis system. The radius of the innermost circle of the family of the concentric circles was 100 μm. It was chosen in such a way that the circle covered at least one average gland-like structure located close to the center of the visual field. In spite of the distorted shape of gland-like structures in adenocarcinomas, the similar size range of those structures allowed the use of the same grid. If the gland-like structure was cut by a circle into two parts, the structure was ascribed to the smallest circle covering its entire area, and counted only once.

One hundred was chosen as the optimal number of samples for the described experiments and statistical analysis of results.

Fractal dimension was calculated for each sample from the radial distribution of the gland-like structures. The numerical experimental data were fitted to the equation of linear regression $\log y(x) = \log a + b \log x$, in which y is a number of gland-like structures within a circle of the grid with a given radius x, a is a scaling coefficient, and b is fractal dimension using software Sigma Plot version 4.0 (SPSS Inc. USA). Arbitrarily, a square root of 2 was applied as the base of all logarithms [15]. Then, the mean value of the parameter b for the 100 samples in each statistical group was calculated. Table II exemplifies distribution of the mean values of the fractal dimension b in adenocarcinomas (G1) and (G2). SD is

shown in the separate column. The significance of difference between the statistical groups was compared according to unbiased test of F statistics and ANOVA algorithm based upon Tukey B test at the confidence value $\alpha = 0.05$ using software Microsoft Excel version 5.0 (Microsoft Corp., Seattle, WA).

RESULTS

The Nucleo/cytoplasmic Ratio and Nuclear Area of Cancer Cells Remain Within the Same Range in Well-Differentiated and Moderately Differentiated Adenocarcinomas

Neither the difference of the nucleo/cytoplasmic ratio, nor the difference of nuclear area between the adenocarcinoma subtypes, is significant (ANOVA, $F^0 = 0.791 < F_\alpha = 3.84$, $P = 3 \times 10^{-3}$ and $F^0 = 0.077 < F_\alpha = 3.84$, $P = 10^{-6}$, respectively, n = 100 sections, k = 20,000 cells, $\alpha = 0.05$). In other words, transformed cells present in gland-like structures of the adenocarcinoma subtypes possess their linear sizes within the same range of values, and, therefore, the same geometry (Table II). In addition, those cells have a well-defined profile of markers (see Materials and Methods, and Table I).

Distribution of Gland-Like Structures Possesses Fractal (Non-Integer) Dimension

As expected, the coefficient of linear regression characterizing a relationship between a number of gland-like structures distributed on a given area of tumor tissue and the radius of a grid has been a noninteger number. No exception from this rule has been found (Table II). In the case of well-differentiated adenocarcinomas (G1), the average fractal dimension is 1.585 (n = 100 sections, SD = 0.038). In the case of moderately differentiated adenocarcinomas (G2), the average fractal dimension is 1.340 (n = 100 sections, SD = 0.044).

Fractal Dimension Reflects Tumor Grading

A difference between the average fractal dimension calculated for both groups of adenocarcinomas is significant (ANOVA, $F^0 = 3.94 > F_\alpha = 0.693$, n = 100 sections, $P = 2 \times 10^{-3}$, $\alpha = 0.05$). The distribution of the gland-like structures is scale invariant and fits the regression curve well. The lowest value of the parameter calculated in this study was 1.052, corresponding to the relatively poor network of gland-like structures in a section of the moderately differentiated adenocarcinoma (G2). A maximum value of 1.829 was calculated for the case of evenly distributed gland-like structures in a relatively homogenous well-differentiated adenocarcinoma (G1).

There Is a Significant Variability of Fractal Dimension Between Consecutive Tumor Tissue Sections

Results of the ANOVA test point out that the values of fractal dimension for well-differentiated adenocarcinomas (G1) and their consecutive sections are within the same range (ANOVA, $F^0 = 1.9856 < F_\alpha = 2.3263$, n = 100 sections, $P = 0.021$, $\alpha = 0.05$). On the contrary, moderately differentiated adenocarcinomas (G2) reveal much higher variability of the parameter between the consecutive tumor sections, which is significant (ANOVA, $F^0 = 1.9856 > F_\alpha = 1.4262$, n = 100 sections, $P = 0.189$, $\alpha = 0.05$).

TABLE II. The Average Values of Nuclear Area (NA), Nucleo-Cytoplasmic Ratio (N/C), and Fractal Dimension (F_D) in Human Gallbladder Adenocarcinomas

Tumor	NA [μm2]	SD	N/C	SD	F_D	SD
ACa G1						
1	59.9	6.8	0.402	0.029	1.519	0.081
2	63.4	5.2	0.409	0.038	1.525	0.031
3	57.9	4.7	0.396	0.034	1.623	0.090
4	61.2	4.6	0.391	0.026	1.623	0.130
5	60.3	7.1	0.392	0.035	1.571	0.044
6	56.9	6.9	0.394	0.041	1.602	0.088
7	62.8	6.5	0.391	0.032	1.569	0.049
8	64.1	5.7	0.393	0.027	1.599	0.103
9	58.7	4.3	0.382	0.021	1.621	0.057
10	61.6	3.9	0.394	0.044	1.596	0.069
Mean	60.7	2.4	0.394	0.007	1.585	0.038
ACa G2						
1	63.5	4.7	0.418	0.022	1.306	0.125
2	62.7	5.2	0.411	0.031	1.383	0.161
3	64.2	6.8	0.398	0.027	1.305	0.061
4	56.1	3.9	0.408	0.035	1.274	0.080
5	61.5	5.8	0.391	0.024	1.338	0.086
6	58.7	5.5	0.421	0.032	1.420	0.115
7	56.9	4.8	0.390	0.029	1.308	0.081
8	61.4	5.9	0.389	0.026	1.336	0.152
9	60.8	6.3	0.421	0.021	1.355	0.126
10	59.6	4.3	0.392	0.038	1.373	0.129
Mean	60.5	2.7	0.405	0.013	1.340	0.044

(ACa) G1 and G2; SD, standard deviation at n = 100 sections and k = 20,000 cells for the mean value, and n = 10 sections and k = 2,000 cells for the individual tumors.

DISCUSSION

A lively debate has located both physical and biological systems within the science of complexity and nonlinearity [16–23]. Eventually, it became apparent that three-dimensional Euclidean geometry only approximates natural objects. In particular, phenomena with nonlinear dynamics possess structural representation known as fractal geometry. A discovery of fractal dimension or a power law, its algebraic analogue, in a number of natural objects—either at the cosmic or microscopic scale—spans a variety of dynamic, nonlinear natural phenomena "...ranging from the surface texture of sea beds, the distribution of intervals between earthquakes, or the structure of star clusters to biological patterns, objects, and phenomena such as cellular metabolism, architecture of normal blood vessels, lung bronchi, or distribution of

pancreatic islets" [8] (also reviewed in [23]). This paper reports that distribution of gland-like structures in gallbladder adenocarcinomas belongs to the same category. The distribution is not utterly random. It is subordinated to the power law with noninteger coefficients possessing fractal regularity as if tumor tissue architecture has actually been intermediate between a one-dimensional object and a two-dimensional surface. To illustrate the above statements, one must imagine a square of side z. Then, the average number of gland-like structures scales for well-differentiated and moderately-differentiated adenocarcinomas as $z^{1.58}$ and $z^{1.34}$, respectively, instead of the expected z^2.

Results of this study demonstrate clearly that fractal dimension describing distribution of gland-like structures is independent of any static cellular category—either geometric, or molecular. While cancer cells present in the tumor tissues analyzed have similar linear sizes and immunohistochemical features [1,2], there is a difference in the fractal dimension between well-differentiated and moderately differentiated adenocarcinomas. The existence of fractal geometry in the adenocarcinomas could simply be ascribed to fractal regularity of blood vessel supply or diffusion of a hormone [24,25]; however, the intra- and intercellular dynamics certainly plays a role in self-emergence of cellular organization [20–22, 26]. Fractal dimension is a holistic parameter which reflects complexity of the interactive system linking its geometry with dynamics. It also reflects the coexistence of deterministic and nondeterministic cellular events; a fact best exemplified by the quasi-deterministic relationship between genotype, a static category, and cellular phenotype, a dynamic category [20,22]. From this perspective, a tissue system comprising the interacting quasi-deterministic units, either normal or malignant, self-emerges and self-organizes rather than develops as a result of interaction between environmental randomness and genetic determinism. Since the increasing number of alterations—a hallmark of tumorigenesis—changes connectivity, redundancy, and complexity within the dynamic cellular network of genes and their regulatory protein elements, a value of fractal dimension also changes [20,22].

In spite of the progressing disorder of tumor tissues, there is fractal regularity in distribution of gland-like structures. In general, decomplexification of the dynamic cellular network can produce decreasing or increasing values of fractal dimension. The lower values of fractal dimension usually denote that the underlying process has slower dynamics. Results of this study suggest that the lower values of fractal dimension correspond to the less advanced organization of adenocarcinomas, which is usually associated with more aggressive and less favorable course of the disease at the organism level. This seemingly paradoxical finding can be explained by the concept of uncoupling between different levels of biological hierarchy in the course of tumorigenesis. In other words, cancer cells undergo decomplexification (i.e., they lose feedbacks normally existing between gene systems, their regulatory elements, signaling pathways, and membrane receptors, etc.). Consequently, uncoupling between microscopic-scale processes such as gene expression, and macroscopic-scale cellular phenomena such as proliferation, differentiation, or apoptosis, occur. The lower values of fractal dimension in moderately differentiated adenocarcinomas (G2) compared to those in well-differentiated adenocarcinomas (G1) denote that the intra- and intercellular interactions within the first tissue system possess lower fractal dynamics (i.e., are weaker, slower, shorter, and less stable). This means that uncoupling between the cellular and tissue level in the population of adenocarcinoma (G2) cells is greater than in the second population of adenocarcinomas (G1). Furthermore, lower intra- and intercellular dynamics implies that cancer cells of adenocarcinomas (G2) are unable to interact collectively at the tissue level to the same extent as cells of the second population, and, therefore, are more independent of each other.

So far, tumor grading system is based upon morphological criteria (i.e., upon the subjective comparison of the morphological patterns in tumor tissues with their normal counterparts). Therefore, the same tumor can be classified in a different manner by histopathologists depending upon their personal experience. For this reason, any comparison of patients, prognoses, treatments, etc., in which tumor grading is important information, cannot be accurate. Fractal dimension and box-counting method can be applied to design a quantitative, objective system of tumor grading. Although fractal analysis is an advanced mathematical tool, both collecting and processing data is quite easy. It can also be carried out with less advanced equipment than computer-aided image analyzer. Fractal dimension can be determined by the alternative methods analyzing whether a number of gland-like structures of the area greater than or equal to a given value fits the curve of the linear regression, calculating the fractal exponent of the relationship between area and perimeter of the gland-like structures [8], or calculating the fractal dimension of heterogeneous spatial structures by the relative dispersion method, which is robust for a low number of data points [27]. With the two latter methods, the study can be performed even if the number of gland-like structures is low (e.g., in poorly differentiated adenocarcinomas). Also, distribution of cancer cells dispersed within tumor stroma can be evaluated by box-counting method. In such a case (i.e., when cancer cells do not form any tissue structures of the higher order), it can be expected that fractal dimension will tend to approach integer values: a situation reflecting a total loss of collective interactions in the population of cancer cells

and possible lack of sensitivity to any extrasystemic therapeutic manipulations (data unpublished).

The qualitative grading neglects a variable geometry of the heterogenous tumor tissue. This study reports the existence of strong variability of the parameter between consecutive tumor tissue sections (i.e., the existence of multiscaling [8]). This local variability reminds one of a vector field with a turbulent flow, which is far from any stationary state. While that field cannot be described in the analytical manner (i.e., by equations), due to the irregular turbulences, it can be characterized by a number of the local and temporary tensors representing strength, direction, orientation, spin, etc. Similarly, each area across tumor tissue possesses different fractal dimension of distribution of the morphological patterns. The geometric variability of tumor architecture would, therefore, be described more accurately in the novel quantitative tumor grading system by a series of fractal dimensions calculated for several consecutive tissue sections rather than by a subjective grade ascribed arbitrarily to the entire tumor. Subsequently, those values characterizing the multiscaling nature of the malignant tumor analyzed should be compared to the scale of reference (i.e., the average values of the parameter determined statistically during the pragmatic study for each representative tumor type and grade). In this way, fractal analysis of tumor sections would provide relevant, statistically reliable, and comparable information for clinicians as to natural, spontaneous evolution of both fractal dynamics and multiscaling in populations of cancer cells originating from a given cell type in the course of a variety of genetic defects.

Such analysis can be performed first at the organism level by computer-aided image analysis of CT scans or high resolution NMR images, and, finally, at the tumor level by image analysis of tumor tissue sections [28–30]. Evolution of cellular dynamics within the tumor and metastases could thus be easily known from those numerical data. It should also be possible to select a cohort of patients with positive responses of cancer cell populations to pharmacological or hormonal interventions, and to observe how fractal dimension changes with the emergence of resistance in the course of adjuvant therapy or spread of metastases. In the latter case, multifractality (i.e., the existence of distinct values of fractal dimension for different dynamic tissue conditions such as various concentrations of a given hormone, tumor marker, or amount of genetic defects [8]) can appear. Multifractality was not observed in the current study because the project has been designed to compare relatively homogeneous groups of tumor tissues. More specific research project at the interface of clinical oncology and tumor pathology is necessary to answer that important question, and to analyze consequences of the possible multifractality for the quantitative system of tumor grading.

ACKNOWLEDGMENTS

The author thanks Professor Sir Colin Berry of the Department of Morbid Anatomy, The London Hospital, London, England; Dr. Christine Bloch of the Department of Neurology, The Cleveland Clinic Foundation, Ohio; and Professor Jerzy Konarski of the Department of Theoretical Chemistry for friendly help, equipment, and multiple discussions.

REFERENCES

1. Albores-Saavedra J, Henson DE, Sobin LH (eds): "Histological Typing of Tumors of the Gallbladder and Extrahepatic Bile Ducts." Berlin: Springer-Verlag, 1991.
2. Nakajo S, Yamamoto M, Tahara E: Morphometric analysis of gallbladder adenocarcinoma: discrimination between carcinoma and dysplasia. Virchows Arch A Pathol Anat Histopathol 1989;416(2):133–140.
3. Nakajo S, Yamamoto M, Tahara E: Morphometrical analysis of gall-bladder adenoma and adenocarcinoma with reference to histogenesis and adenoma-carcinoma sequence. Virchows Arch A Pathol Anat Histopathol 1990;417(1):49–56.
4. Sedivy R: Fractal tumours: their real and virtual images. Wien Klin Wochenschr 1996;108(17):547–551.
5. Sandau K, Kurz H: Measuring fractal dimension and complexity—an alternative approach with an application. J Microsc 1997;186(2):164–176.
6. Schwartz D, Lellouch J: Explanatory and pragmatic attitudes in therapeutical trials. J Chron Dis 1967;20:637–648.
7. Murray GD: Statistical aspects of research methodology. Br J Surg 1991;78:777–781.
8. Hastings HM, Sugihara G (eds): "Fractals. A User's Guide for the Natural Sciences." Oxford: Oxford University Press, 1993.
9. Dahiya R, Kwak KS, Byrd JC: Mucin synthesis and secretion in various human epithelial cancer cell lines that express the MUC 1 mucin gene. Cancer Res 1993;53:1473–1443.
10. De Boer WG, Ma J, Rees JW: Inappropriate mucin production in gallbladder metaplasia and neoplasia—an immunohistological study. Histopathology 1981;5:295–303.
11. Gum JR Jr: Mucin genes and the proteins they encode. Structure, diversity and regulation. Am J Respir Cell Mol Biol 1992;7(6): 557–564.
12. Yamaguchi K, Enjoji M: Carcinoma of the gallbladder. A clinicopathology of 103 patients and a newly proposed staging. Cancer 1988;62:1425–1432.
13. Yamamoto M, Nakajo S, Tahara E: Carcinoma of the gallbladder: the correlation between histogenesis and prognosis. Virchows Arch A Pathol Anat Histopathol 1989;414(2):83–90.
14. Culling CF, Allison RT, Barr WT (eds): "Cellular Pathology Technique." London: Butterworths, 1985.
15. Hastings HM, Schneider BS, Schreiber M, et al.: Statistical geometry of pancreatic islets. Proc Royal Soc Lond Ser B 1992;250: 257–261.
16. Haken H: "Synergetics: An Introduction." Berlin: Springer-Verlag, 1978.
17. Rosen R: Organisms as causal systems which are not mechanisms: An essay into the nature of complexity. In Rosen R (eds): "Theoretical Biology and Complexity." Orlando: Academic Press, 1985: 165–203.
18. Rubin H: Adaptive evolution of degrees and kinds of neoplastic transformation in cell culture. Proc Natl Acad USA 1992;89:977–981.
19. Stein DL (ed): "Lectures in the Sciences of Complexity. Vol. 1." Santa Fe: Addison-Wesley, 1989.
20. Waliszewski P: Complexity, dynamic cellular network, and tumorigenesis. Pol J Path 1997;48(4):235–241.
21. Sedivy R, Mader RM: Fractals, chaos, and cancer: Do they coincide? Cancer Investig 1997;15(6):601–607.

22. Waliszewski P, Molski M, Konarski J: On the holistic approach in cellular and cancer biology: Nonlinearity, complexity, and quasi-determinism of the dynamic cellular network. J Surg Oncol 1998; 68:70–78.
23. Mandelbrot BB: "The Fractal Geometry of Nature." San Francisco: Freeman, 1983.
24. Peitgen HO, Jurgens H, Saupe D (eds): "Chaos and Fractals. New Frontiers of Science." New York: Springer-Verlag, 1992:183–228.
25. Witten TA, Sander LM: Diffusion-limited aggregation, a kinetic critical phenomenon. Phys Rev Lett 1981;47:1400–1403.
26. Sernetz M, Gelleri B, Hofman F: The organism as a bioreactor; interpretation of the reduction law of metabolism in terms of heterogenous catalysis and fractal structure. J Theor Biol 1985; 117:209–230.
27. Bassingthwaighte JB, Liebovitch LS, West BJ (eds): "Fractal Physiology." Oxford: Oxford University Press, 1994:72–77.
28. Peiss J, Verlande M, Ameling W, et al.: Classification of lung tumors on chest radiographs by fractal texture analysis. Invest Radiol 1996;31(10):625–629.
29. Lucht R, Brix G, Lorenz WJ: Texture analysis of differentially reconstructed PET images. Phys Med Biol 1996;41(10):2207–2219.
30. Beier J, Liebig T, Bittner RC, et al.: Fractal surface analysis of intrapulmonary space-occupying lesions from high-resolution CT studies. Neuen Bildgeb Verfahr 1997;166(4):296–302.